

## Fiber modulators and fiber amplifiers for LISA

This content has been downloaded from IOPscience. Please scroll down to see the full text.

2010 J. Phys.: Conf. Ser. 228 012042

(<http://iopscience.iop.org/1742-6596/228/1/012042>)

View [the table of contents for this issue](#), or go to the [journal homepage](#) for more

Download details:

IP Address: 194.95.157.184

This content was downloaded on 26/04/2017 at 10:52

Please note that [terms and conditions apply](#).

You may also be interested in:

[Auxiliary functions of the LISA laser link](#)

Gerhard Heinzl, Juan José Esteban, Simon Barke et al.

[Ranging and phase measurement for LISA](#)

Juan José Esteban, Antonio F García, Johannes Eichholz et al.

[Fiber laser development for LISA](#)

Kenji Numata, Jeffrey R Chen and Jordan Camp

[Towards a Suspension Platform Interferometer for the AEI 10 m Prototype Interferometer](#)

K Dahl, A Bertolini, M Born et al.

[The gravitational wave observatory designer: sensitivity limits of spaceborne detectors](#)

S Barke, Y Wang, J J Esteban Delgado et al.

[A demonstration of LISA laser communication](#)

S E Pollack and R T Stebbins

[Noise sources in the LTP heterodyne interferometer](#)

V Wand, J Bogenstahl, C Braxmaier et al.

[Precision laser development for interferometric space missions NGO, SGO, and GRACE Follow-On](#)

K Numata and J Camp

[Picometer interferometry for the LISA gravitational reference sensor](#)

Thilo Schuldt, Martin Gohlke, Dennis Weise et al.

## Fiber modulators and fiber amplifiers for LISA

M Tröbs<sup>1</sup>, S Barke<sup>1</sup>, J Möbius<sup>2,3</sup>, M Engelbrecht<sup>2,4</sup>, Th Theeg<sup>2</sup>,  
D Kracht<sup>2</sup>, B Sheard<sup>1</sup>, G Heinzl<sup>1</sup> and K Danzmann<sup>1</sup>

<sup>1</sup> AEI Hannover, (MPI für Gravitationsphysik und Leibniz Universität Hannover), Callinstr.  
38, 30167 Hannover, Germany

<sup>2</sup> Laser Zentrum Hannover, Hollerithallee 8, 30419 Hannover, Germany

<sup>3</sup> present address: Viscom AG, Carl-Buderus-Straße 9-15, 30455 Hannover, Germany

<sup>4</sup> present address: Menlo Systems GmbH, Am Klopferspitz 19, 82152 Martinsried (Munich),  
Germany

E-mail: michael.troeb@aei.mpg.de

**Abstract.** We present the sideband phase characteristics of a fiber-coupled integrated electro-optical modulator (EOM) at a modulation frequency of 2 GHz for Fourier frequencies from 0.1 mHz to 1 Hz. The upper phase noise limit was almost an order of magnitude better than required for LISA. The EOM's phase dependencies on temperature and transmitted optical power were measured and found to be uncritical. Additionally we have investigated three optical amplifiers emitting 1 W. Their differential phase noise and optical pathlength noise as one contribution to differential phase noise were measured. The measured differential phase noise was within the requirement. The dependencies of differential phase noise on pump power were measured and requirements for the operation of the amplifier on the LISA satellite derived.

### 1. Introduction

In the LISA mission [1] the phase of the beat note between pairs of laser beams will be measured to detect pathlength variations caused by gravitational waves. Each satellite requires a stable frequency standard (ultra-stable oscillator, USO) for this phase measurement. There are no suitable space-qualified frequency standards known to the authors providing the required accuracy. Due to the Doppler shift resulting from the relative velocities of the spacecraft (S/C), the beat notes lie between 2 and 20 MHz. To reach the required sensitivity the clock noise must be removed in post-processing [2]. Electro-optical modulators (EOMs) will be used to imprint the clock noise of the local USO as phase modulation sidebands onto the laser beam travelling to the remote spacecraft where this clock noise will be compared to the local clock noise. The differential clock noise will be recorded and sent to Earth for post-processing. No component in the clock noise transfer chain may degrade the phase fidelity of the phase modulation sidebands with respect to the carrier.

We have investigated the phase fidelity of two components in the clock noise transfer chain, namely an EOM and three fiber amplifiers (FAs). The requirements for EOM and fiber amplifier differential phase noise used here are based on  $1 \text{ pm}/\sqrt{\text{Hz}}$  equivalent displacement noise at the heterodyne frequency. By using a high modulation frequency  $f_{\text{SB}}$  for the EOM sidebands to be transmitted through the amplifier, the phase noise requirement between carrier and sideband is relaxed by the factor  $f_{\text{SB}}/f_{\text{het}}$  where  $f_{\text{het}} = 2 \dots 20 \text{ MHz}$  is the heterodyne frequency onboard

the LISA spacecraft. In our case with  $f_{\text{SB}} = 2 \text{ GHz}$  this results in a differential phase noise requirement  $\phi_{\text{RQ}}$  of

$$\phi_{\text{RQ}}(f) = 0.6 \frac{\text{mrad}}{\sqrt{\text{Hz}}} \cdot \sqrt{1 + \left(\frac{2.8 \text{ mHz}}{f}\right)^4} \quad (1)$$

where the commonly used frequency shape factor has been used [3, 4, 5].

## 2. EOM single sideband phase characteristics

We have investigated an integrated optical phase modulator based on LiNbO<sub>3</sub> / MgO:LiNbO<sub>3</sub> crystals for wavelengths of  $1064 \text{ nm} \pm 60 \text{ nm}$  [6]. The phase of the light could be modulated with frequencies ranging from 100 Hz to 2 GHz. At 2 GHz modulation frequency the half-wave voltage measured 8.6 V. The modulator could handle up to 300 mW of optical power with a 4 dB insertion loss and was equipped with polarisation maintaining single-mode fibers.

### 2.1. EOM single sideband phase noise

In contrast to Klipstein et al. [3] who measured the relative phase noise between the sidebands of two EOMs, we have chosen a setup which allowed us to investigate the phase noise of a single EOM. The setup is shown in Fig. 1. Two laser beams were superimposed at a beam splitter with one beam first sent through an EOM driven by a 2 GHz + 1.6 kHz signal. Both then were passed through a mode cleaning fiber (not shown in the schematic setup) and sent to two photodiodes. The beatnote signal of one photodiode was mixed with a 2 GHz reference signal, low-pass filtered and used to offset phase lock both lasers to the reference frequency. At the other photodiode, we measured the carrier-carrier beat note at 2 GHz, mixed it down using the EOM driver signal and low-pass filtered the output. In the end the phase of the resulting 1.6 kHz signal was measured by a software phasemeter operating with the same principle as the phasemeter of the LISA Technology Package (LTP) [7]. The phase of the sideband-carrier beat note at 1.6 kHz which contained phase shifts induced by the EOM was also measured. To remove setup noise such as residual phase lock error and phase noise of the EOM driver signal, we subtracted the phase of the mixed-down carrier-carrier signal from the sideband-carrier beat.

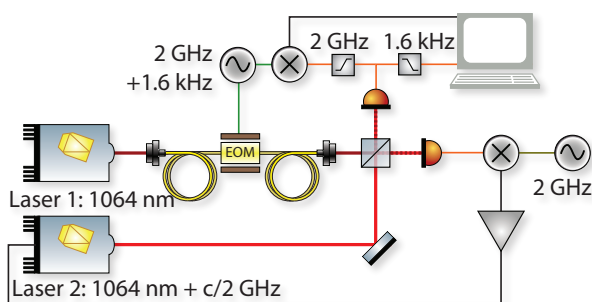


**Figure 1.** Schematic setup for EOM phase noise measurements.

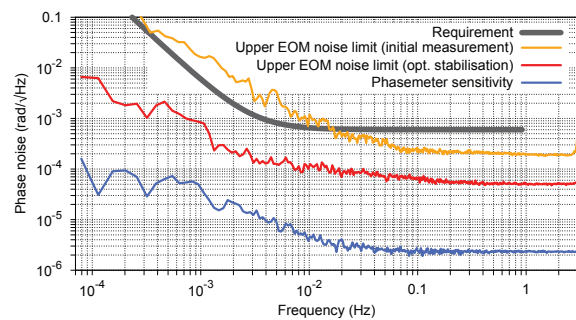


**Figure 2.** Differential phase noise measurement.

Figure 2 shows the measurement results. We showed that the upper phase noise limit of the EOM (red trace) was almost an order of magnitude better than the LISA mission requirements (grey trace). For this measurement the 2 GHz beat-note power was stabilized to a constant reference by tuning the laser power (pump diode current). This technique removed power-level related phase shifts in the electronic mixers that were visible in the initial measurement that

was performed without this stabilization (yellow trace). The program LPSD [8, 9] was used to generate the traces shown in Fig. 2 and in all following graphs showing spectral densities.

### 2.2. Dependencies of EOM phaseshift on temperature and light power

We measured the dependency of the relative phase between the carrier and one sideband generated inside the EOM on the temperature. For doing so we placed the EOM in an aluminium housing with thermo-electric coolers (TEC) attached to it. Platinum resistors in the aluminium housing were used to measure the EOM temperature. While the EOM temperature was varied, the resulting phase shift was recorded using the setup shown in Fig. 1. Figure 3 shows the measurement result of the phase shift induced by the EOM versus its temperature (red for heating and orange for cooling periods). A linear fit is shown in blue which represents a dependency of  $2.1 \pm 0.2$  mrad/K.

The temperature of the output fiber of the EOM was also altered and the resulting phase shift between carrier and sideband was measured to be  $1.5 \pm 0.2$  mrad/K for the 1.5 m long output fiber. Combining both coefficients we obtained a total phase dependency on the EOM's temperature of about 3.6 mrad/K.

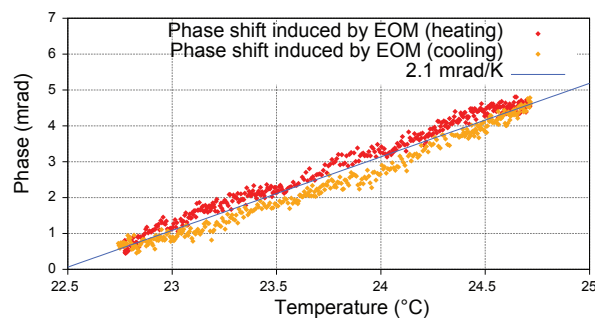


**Figure 3.** Measured dependency of EOM phasenoise on temperature.

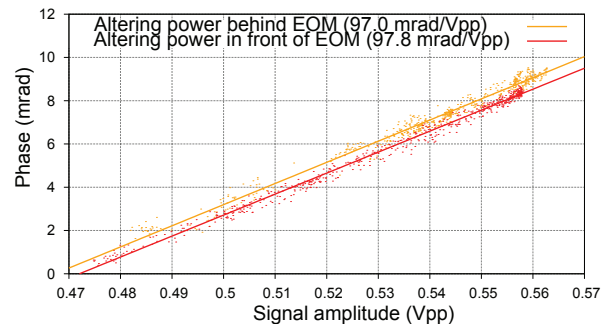


**Figure 4.** Measured dependency of EOM phasenoise on optical power.

We have also determined the photorefractive effect (phase dependence on transmitted optical power) by altering the laser power going through the EOM. Figure 4 shows the differential phase plotted against the beat signal amplitude. The optical input power was varied by detuning the fiber coupling to the EOM and the resulting phase shift between carrier and sideband was measured (red trace). Since altering the laser power causes phase shifts not only in the EOM but also in e.g. the mixer, we have made a second measurement where the optical power behind the EOM was varied by detuning the coupling to the mode cleaning fiber and the resulting phaseshift was measured (yellow trace). The influence of the EOM—and hence the photorefractive effect—is the difference between the slope coefficients of the two traces; this was computed to be  $0.0026 \pm 0.0022$  mrad/mW.

Both, the phase dependency of the EOM on temperature and on optical power is compatible with the expected noise levels onboard the LISA satellites.

### 3. Fiber amplifier phase stability

In previous experiments [10, 11] the length noise of a fiber amplifier was measured. First measurements of phase noise between carrier and sideband on fiber amplifiers have been reported in [5].

### 3.1. Amplifiers under test

We have investigated three Ytterbium-doped fiber amplifiers emitting 1 W of output power that were pumped by diode lasers at 976 nm in the direction of the seed beam.

The first amplifier consisted of two identical stages using 0.4 m polarization-maintaining (PM) Yb-doped single-mode fiber with 490 dB/m absorption at the pump wavelength and 5.7  $\mu\text{m}$  core diameter by INO. It was not fully polarization-maintaining since non-PM wavelength division multiplexers (WDMs) were used to couple the pump light in the active fiber. This amplifier will be called core-pumped amplifier (CPA) in the following. It was seeded with 30 mW and pumped by approximately 2 W.

The second amplifier consisted of a single stage using 3 m Yb-doped double-clad fiber (Yb1200-10/125DC-PM by Liekki) with a 10  $\mu\text{m}$  core diameter, a 125  $\mu\text{m}$  cladding diameter, and numerical apertures of 0.08 and 0.46 for the core and pump cladding, respectively. It was fully polarization-maintaining and the pump diode was cooled by a fan. This amplifier will be called double-clad amplifier 1 (DCA1). It was seeded by 45 mW and pumped by 3.5 W.

The third amplifier also consisted of a single stage using 7.5 m Yb-doped double-clad fiber (PM-YDF-5/130 by Nufern) with a 5  $\mu\text{m}$  core diameter, a 130  $\mu\text{m}$  pump cladding diameter, and numerical apertures of 0.13 and 0.46 for the core and pump cladding, respectively. The amplifier was fully polarization-maintaining. The pump diode was placed on a heat sink with thermoelectric cooling without fans. This amplifier will be called double-clad amplifier 2 (DCA2). It was seeded by 40 mW and pumped by 2.3 W. The seedpowers that were used are in the output power range of the LISA Pathfinder laser, that emits 45 mW and is forseen as seed source for a fiber amplifier within LISA.

### 3.2. Optical pathlength noise measurements

Optical pathlength changes in an amplifier,  $\Delta s$ , due to e.g. changes in ambient temperature, pump power, or seed power lead to differential phase changes,  $\Delta\phi$ , of sidebands at  $f_{\text{SB}}$  with respect to the carrier of

$$\Delta\phi = \frac{2\pi f_{\text{SB}}}{c} \Delta s, \quad (2)$$

where  $c$  is the speed of light in vacuum. We have measured the length noise of the three amplifiers with the setup shown in Fig. 5 and used Eq. (2) to calculate the effect of amplifier length changes on phase noise between carrier and a 2 GHz sideband. The amplifier under test

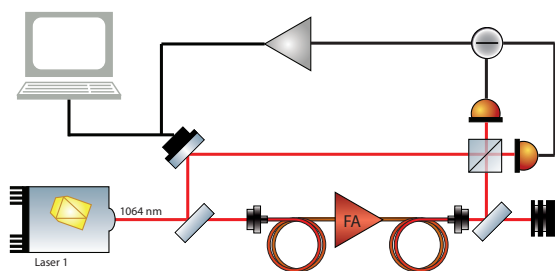


**Figure 5.** Simplified setup to measure fiber amplifier length noise.

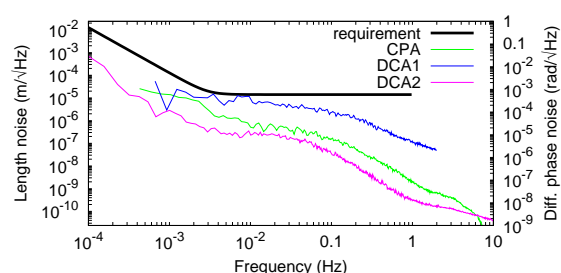


**Figure 6.** Measured length noise of the fiber amplifiers.

was placed in one arm of a homodyne Mach-Zehnder interferometer. The output phase was detected with a balanced detector and stabilized on mid-fringe by acting on a PZT-mounted mirror in the other arm. The calibrated actuator signal was used as measure for the amplifier length noise. The setup was enclosed in a thermal shield made of extruded polystyrene. The amplifiers were covered with an additional thermal isolation layer.

Figure 6 shows the measured optical pathlength noise of the fiber amplifiers on the left axis. The right axis shows the projected differential phase noise between carrier and a 2 GHz sideband caused by the optical pathlength noise as given by Eq. (2). All three amplifiers showed lower optical pathlength noise for higher Fourier frequencies. Double-clad amplifier 1 showed the highest optical pathlength noise of the three amplifiers. It touched the requirement between 3 mHz and 10 mHz. The core-pumped amplifier and double-clad amplifier 2 showed lower optical pathlength noise than double-clad amplifier 1, at 10 mHz by factors of 10 and 20, respectively. The optical pathlength noise depends on fiber length, the type of fiber and its jacketing [12], pump power noise, seed power noise, and ambient temperature noise. The three amplifiers consisted of different lengths and types of fibers and used different pump diodes. The fan used within DCA1 but not within CPA and DCA2 might be a cause for the higher length noise.

### 3.3. Differential phase noise measurements

Figure 7 shows the simplified experimental setup used for measuring differential phase noise. Light from two lasers was interfered at a beam splitter and detected by a (fiber-coupled) photodiode. A control loop was used to offset-phase lock the lasers with a 2 GHz frequency difference. The same photodiode signal and that of a (fiber-coupled) photodiode behind the amplifier were mixed with a 2 GHz + 1.6 kHz local oscillator. The phases of the resulting 1.6 kHz signals were measured using a LISA Pathfinder-style phasemeter [7], that was implemented using a PC with DAQ card and self-written software. Since the mixers showed a signal amplitude dependent phase shift, the amplitudes of the 1.6 kHz signals were stabilized by acting on the light power incident on the photodiodes by PZT-mounted tilting mirrors that altered the coupling efficiency to the fiber-coupled photodiodes. The setup was again enclosed in a thermal shield made of extruded polystyrene and the amplifier under test was covered with an additional isolation layer.

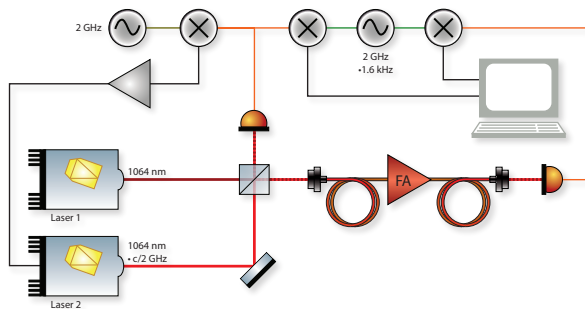


**Figure 7.** Simplified setup to measure fiber amplifier differential phase noise.

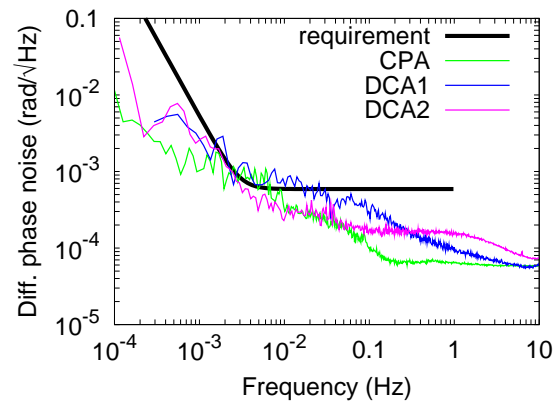


**Figure 8.** Measured differential phase noise of the fiber amplifiers.

Figure 8 shows the measured differential phase noise for the three amplifiers. All amplifiers showed differential phase noise within the LISA requirement. Between 3 mHz and 10 mHz double-clad amplifier 1 was limited by optical pathlength noise, the other two differential phase noise measurements were limited by setup noise (traces not shown).

### 3.4. Dependencies of differential phase on pump power

Dependencies of differential phase on pump power were measured. The strongest measured dependencies and resulting noise requirements are shown in Table 1. While the two double-clad

**Table 1.** Measured strongest dependencies of differential phase noise on pump current and resulting noise requirements.

Parameter	Unit	CPA	DCA1	DCA2
Diff. phase / pump power	(mrad/W)	32	58	161
Noise requirement	(mW/ $\sqrt{\text{Hz}}$ )	18	10	4

amplifier used one pump diode each, the core-pumped amplifier used four pump diodes. For the measurement, three pump diodes were operated at constant power, while one pump diode power was changed and the differential phase was measured. With increasing length of the active fiber, the coefficient from pump power to differential phase increased. The noise requirements shown in Table 1 each result in differential phase noise at the requirement. When multiple operating parameters are taken into account and requirements for them are made, a suitable noise budget has to be allocated to each noise source such that the combined effect results in differential phase noise within the overall requirement.

#### 4. Conclusions

In conclusion, we have measured an upper limit to the phase noise introduced by an EOM between carrier and a 2 GHz sideband and found this phase noise to be almost one order of magnitude below the requirement. The dependency of EOM phase shift on temperature of 3.6 mrad/K and on optical power of  $0.0026 \pm 0.0022$  mrad/mW were measured.

Three fiber amplifiers emitting 1 W were investigated. For all fiber amplifiers the phase noise between carrier and 2 GHz sideband was within the requirement. Optical pathlength noise as one source of differential phase noise was measured for the three amplifiers. Only the differential phase noise of double-clad amplifier 1 was limited by its optical pathlength noise for Fourier frequencies between 3 mHz and 10 mHz. Maximum dependencies of differential phase noise on pump power were measured. None required the use of an active pump power stabilization.

#### Acknowledgments

We acknowledge support by Deutsches Zentrum für Luft- und Raumfahrt (DLR) (reference 50 OQ 0601) and thank the German Research Foundation for funding the Cluster of Excellence QUEST – Centre for Quantum Engineering and Space-Time Research.

#### References

- [1] Danzmann K and Rüdiger A 2003 *Class. Quantum Grav.* **20** S1–S9
- [2] Hellings R W 2001 *Phys. Rev. D* **64** 022002
- [3] Klipstein W, Halverson P G, Peters R, Cruz R and Shaddock D 2006 *LASER INTERFEROMETER SPACE ANTENNA: 6th International LISA Symposium* vol 873 ed Merkowitz S M (American Institute of Physics) pp 312–318
- [4] Barke S, Tröbs M, Sheard B, Heinzl G and Danzmann K 2010 *Appl. Phys. B* **98** 33–39
- [5] Tröbs M, Barke S, Möbius J, Engelbrecht M, Kracht D, d’Arcio L, Heinzl G and Danzmann K 2009 *J. Phys.: Conf. Ser.* **154** 012016
- [6] JENOPTIC Laser, Optik, Systeme GmbH, Jena, Germany Integrated Optical Phase Modulator / Fiber-coupled electro-optical light-modulator <http://www.jenoptik-los.de/cms.php?pageid=788&lang=0>
- [7] Heinzl G, Wand V, Garcia A, Jennrich O, Braxmaier C, Robertson D, Middleton K, Hoyland D, Rüdiger A, Schilling R, Johann U and Danzmann K 2004 *Class. Quantum Grav.* **21** S581–S587
- [8] Tröbs M and Heinzl G 2006 *Measurement* **39** 120–129
- [9] Tröbs M and Heinzl G 2009 *Measurement* **42** 170
- [10] Tröbs M, Weßels P and Fallnich C 2005 *Opt. Lett.* **30** 789–791
- [11] Tröbs M, Weßels P and Fallnich C 2005 *Opt. Express.* **13** 2224–2235
- [12] Tateda M, Tanaka S and Sugawara Y 1980 *Appl. Opt.* **19** 770–773 ISSN 0003-6935